KeAi
CHINESE ROOTS
GLOBAL IMPACT

International Journal of Innovation Studies

THERMAL RADIATION AND HEAT GENERATION EFFECTS ON UNSTEADY MAGNETOHYDRODYNAMIC FREE CONVECTION FLOW PAST AN INFINITE VERTICAL PLATE WITH COUPLED HEAT AND MASS TRANSFER

Vasa Vijaya Kumar[1] , M N Raja Shekar.[2]
Ph.D Research Scholar, Department of Mathematics, JNT University Hyderabad 500085,Telangana,INDIA.[1]
Department of Mathematics, JNTUH University College of Engineering Jagtial, Telangana 505501,INDIA.[2]
* Corresponding Author
Email Address: vasavijayphd@gmail.com

ABSTRACT
Magnetohydrodynamic (MHD) free convection flow with coupled heat and mass transfer plays a vital role in nuclear cooling, polymer processing, and energy systems. However, the combined influence of thermal radiation and internal heat generation on unsteady Casson fluid flow past a vertical plate remains insufficiently explored. To address this limitation, the present study develops a comprehensive mathematical model incorporating magnetic field effects, buoyancy forces, radiation parameter (R), and heat generation parameter (Q). The governing nonlinear partial differential equations are transformed into nondimensional form and solved numerically using the Crank–Nicolson implicit finite difference method with 101 spatial grid points and 200-time steps. Numerical results reveal that increasing the radiation parameter from $R = 0.5$ to $R = 2$ enhances the Nusselt number from −0.055 to −0.042 (≈24% improvement in heat transfer rate). Similarly, peak velocity increases from 1.6 to 4.4 as the thermal Grashof number rises from 2 to 10. Higher Schmidt number reduces concentration boundary thickness significantly. Overall, radiation and buoyancy enhance thermal transport, while magnetic effects suppress velocity, providing valuable insights for thermal system optimization.

Keywords: Magnetohydrodynamics(MHD), Casson Fluid, Thermal Radiation, Heat Generation, Finite Difference Method

1. INTRODUCTION

Magnetohydrodynamics (MHD) is an important interdisciplinary field that studies the behavior of electrically conducting fluids under the influence of magnetic fields. Some examples of such fluids are liquid metals, electrolytes, ionized gases and plasmas [1]. The relationship which exists between fluid dynamic and electromagnetic forces considerably changes the circumstances of transport momentum, heat and mass [2]. The effect of coupling is important in most engineering and industrial operations, including metallurgical operations, crystal growth, cooling of nuclear reactor, extraction of geothermal energy and MHD power generation. Due to its broad scope of practical use, the research of MHD free convection flow has been a point of constant interest among researchers in the last few decades [3].

Free convection flow is initiated by the differences in density, which occurs because of either temperature or concentration gradient in a fluid. As a vertical plate is either heated or

cooled, there would arise forces of buoyancy in the adjoining fluidic layer, which create motion despite no external driving force [4]. When a transverse magnetic field is induced in the fluid and it is a conducting material, then we have the Lorentz forces whose effect is to oppose to the movement of the fluid. This damping force is due to magnetism and it changes the velocity distributions and therefore affects the rate of heat transfer and mass transfer [5]. Such flows are even more important to analyze in the conditions of high temperatures when the effects of thermal radiation cannot be disregarded [6].

In exceptionally high temperature processes, one of the most common modes of heat transfer is thermal radiation which includes process such as combustion systems, gas turbines, re-entry vehicles and astrophysical flows [7]. When this happens, exchange of energy through radiation has a significant influence on the temperature field of the boundary layer. Radiative heat flux causes changes in the thickness of the thermal boundary layer and alteration in the heat transfer rate of the surface [8]. Thus, addition of radiation implications to the math model gives the physical issue a more realistic representation. Internal heat generation or absorption is another factor that is very crucial in most practical systems. The heat can be generated as a result of chemical processes, electrical heating, nuclear processes, and viscous cooling of the fluid [9]. Inclusion of a term, representing a heat source in the energy equation, is found to have significant effect on the temperature field as well as the buoyancy force which propels the flow [10]. Thermal boundary layer could either become thick or thin, depending on the heat generation or absorption, which would cause a change in velocity and concentration profiles. Therefore, the interaction of thermal radiation and heat general is decisive in the studies of realistic convective flow systems [11].

The flow behavior is further complicated by a situation of mass transfer and heat transfer. The coexistence of both thermal and concentration gradients is widely occurring in most industrial uses where time is used in drying, evaporation, chemical processing and dispersion of pollutants [12]. The differences in temperature and species concentration cause the resulting buoyancy forces resulting in the phenomenon of the double-diffusive convection [13]. A combination of the heat and mass transfer process enables one to understand how both thermal and solutal boundary layers interact [14]. This is especially important in environmental engineering, food processing as well as energy systems where diffusion processes determine system performance.

The current research takes into account the issue of unsteady free convection flow over an infinite vertical plate. The plate assumption of infinite size makes the analysis of the flows easier since the plate effect at the edges is removed and the variables of the flow are made to be that of the normal distance between the plate and time only [15]. The unsteady flow analysis is of significance when the temperature or concentration of the surface varies over time as expected in start-up processes, time-dependent heating or time-dependent boundary conditions [16]. In contrast to steady-state problems, unsteady flows also describe how velocity, temperature, and concentration fields change in time, giving a better round picture in the transient transport phenomena [17].

Mathematically, the equations that govern the problem are various coupled and non-linear partial equations that formulate conservation of mass, momentum, energy and species concentration present [18]. Additional complexity to the governing equations comes when trying to include magnetic field, thermal radiations and internal heating. Precise analytical

solutions of these highly coupled non-linear systems are usually not easily to come by [19]. Consequently, mathematical approaches come into play as an important tool to work out these equations in an accurate manner. In this study, we have made use of finite difference technique to discretize and solve the transformed equations. The technique is extremely common because it is simple, stable, and efficient in management of problems of the boundary layer type.

Such studies are of interest in physical quantities related to the velocity, temperature, and concentration fields in the boundary layer, the skin-friction coefficient, the Nusselt number (rate of the heat transfer), and the Sherwood number (rate of the mass transfer) [20]. Skin-friction coefficient is the surface shear stress of the fluid motions. Nusselt number is a measurement of the effectiveness of the plate in terms of heat transfer whereas Sherwood number represents the mass transfer rate [21]. The variation of these parameters with modification of the magnetic field strength, the radiation parameter, the heat generation parameter, the thermal and solutal Grashof equations and Schmidt number is the key to optimization of the engineering system.

The relevance of the current study is that it takes a holistic approach in probing the joint effect of magnetic field, thermal radiation, internal heat generation and heat and mass transfer in an unsteady free convection flow. Applicability of such combined effects in most advanced technological processes such as cooling of electronic devices, nuclear reactors, polymer processing and space technology. The findings of this numerical investigation can be used to learn more about the physics of how the electromagnetic forces interact with the buoyancy-driven convection in a transient scenario. To conclude, the research on the influence of thermal radiation and heat generation on unsteady flow of MHD free convection past an infinitely long vertical plate under heat and mass transport conditions is a demanding theoretical and valuable practical question. The current work helps to gain a more profound insight into the behavior of complex transport phenomena in the electrically conducting fluids by numerically solving the governing equations and analyzing the impact that multiple physical parameters have on them. The results can become a valuable resource to the researchers and engineers that consider designing and analyzing thermal systems in which magnetic fields, as well as radiative heat transfer, are major factors.

2. LITERATURE REVIEW

The recent literature has shown that there is an interest in research investigations on unsteady magnetohydrodynamic (MHD) free convection flows that includes radiation effects, effects of chemical reactions, and porous mediums. For instance, Rabha et al., (2025) [22] explored unsteady MHD free convective micropolar fluid flow when a vertically moving porous plate is subjected to thermal radiation as well as first-order chemical reaction by employing a perturbation technique. Their results showed that the magnetic fields inhibit velocity, radiation cools down, and chemical reactions decrease the concentration level, whereas the radiation increases the rates of heat transfer. In the same manner, Lutera et al., (2025) [23] examined the 7 simulations of the radiative flow of nanofluids on exponentially accelerating surface by the finite difference method, and they noted that the thermal radiations greatly contribute to the velocity and temperature growth. Moreover, Sahu et al., (2025) [24] included points on the thermal and mass stratification by an exact solution of the Laplace transform and proved that stratification reduced the velocity but enhanced the Nusselt and Sherwood numbers. In the same vein, Aroloye et al., (2024) [25] used Runge-Kutta shooting

method to demonstrate that the magnetic parameter, Soret number, Schmidt number and radiation have a considerable effect on distributions of velocity, temperature and concentration. Altogether, these works underline the prevalence of radiation and magnetic forces in the regulation of the features of the boundary layer.

Moreover, non-Newtonian and nanofluid models are being studied to further the knowledge of transport phenomenon in porous media. As reported in Islam et al., (2024) [26], the current study numerically investigated the unsteady MHD Casson fluid flow using finite difference method and found that magnetic effects increase the temperature of a plate as well as change the skin friction and transfer rates. Similarly, Sudarmozhi et al., (2024) [27] investigated the viscoelastic fluid flow of Maxwell equations with radiations and heat generation in the bvp4c solver tool of MATLAB and found that the higher the Rayleigh number, the higher the velocity but the higher the radiation the higher the temperature profiles respectively. In another similar investigation, Das et al., (2024) [28] utilized the Laplace transform approach to achieve closed-form solutions to oscillatory MHD flow and established that the values of radiations and magnetic parameters have an important impact on the Nusselt number and skin friction. In the same way, in (29) Prakash et al., analytically analyzed the flow of fluids in a rotating porous medium, Casson fluid, and indicated retarding effects of heat generation and porous parameters on velocity and temperature. Besides, Reddy et al., (2023) [30] applied finite element method, in their study of nanofluid flow, and found that radiation accelerates velocity and temperature, and magnetic parameters inhibit movement. These papers emphasize the significance of fluid rheology and porous structure in regulating thermal and momentum transport. Moreover, some authors have devoted their attention to thermos diffusion, viscous dissipation, and Hall current effects to increase their practice. The Eckert and Dufour numbers were heavily altered by Hasanuzzaman et al., (2023) [31] when they used the finite difference method in a study that showed these numbers morph the skin friction and the rates of heat transfer. In line with this, Prabhakar et al., (2023) [32] were able to study inclined permeable plates via the DuFort Frankel scheme, and the magnetized plates decreased velocity with increased radiation on the Nusselt number. The investigations by Uddin et al., (2023) [33] proved that under time-dependent flows, radiation on a boundary layer reduces temperature in the said boundary layer, as the radiation increases. Previously, Sarma et al., (2022) [34] have obtained the precise Laplace solutions with Rosseland approximation and found that radiation enhances the amount of heat conveying, whilst decreases the effect of Sorter. Lastly Poddar et al., (2022) [35] numerically investigated the rotating radiative MHD flow using Hall current and stabilized it and convergence by explicit finite difference schemes. Generally speaking, the articles reviewed prove the existence of magnetic field to specifically slow down the movement of liquids, whereas radiation, chemical reaction, stratification, and thermos diffusion play a great role in shaping thermal and concentration gradients. Nonetheless, it can be thought that in advanced industrial and engineering practice, further unified modeling tools can be developed by variations of fluid models, numerical strategies, and boundary conditions.

Although the literature in the unsteady MHD convective flows has been performed extensively, there are still a number of limitations. Majority of existing literature examines single, or a few physical effects including radiation, chemical reaction, or stratification independently, yet, actual industrial systems are multi-physics in nature. Furthermore, most

research works take into account special fluids (Casson, Maxwell, nanofluid, micropolar) in simplified boundary conditions and steady porous systems, which restricts their application to the general case. There is also limited comparison and contrast between analytical and the high-accuracy numerical process. Also, coupled heat and mass transfer behaviour and transient behaviour of thermal transport under complex geometries are not often covered. Thus, a unified framework that combines various mechanisms of transport, variable properties, and lifelike boundary conditions is yet to be developed.

Table 1: Recent MHD Heat and Mass Transfer Studies Comparison

Author (Year)	Flow/Fluid Model	Method Used	Key Parameters Studied	Major Findings
Rabha et al., (2025) [22]	Unsteady MHD micropolar fluid over porous vertical plate with chemical reaction & radiation	Perturbation analytical method	Magnetic field, buoyancy, radiation, Prandtl no., reaction rate	Magnetic field decreases velocity; radiation reduces temperature; chemical reaction lowers concentration; radiation increases heat transfer
Lutera et al., (2025) [23]	Nanofluid flow over exponentially accelerating surface	Finite Difference Method (MATLAB)	Thermal radiation, heat generation, magnetic field	Radiation increases temperature & velocity; heat generation reduces skin friction
Sahu et al., (2025) [24]	Unsteady MHD flow with thermal & mass stratification	Laplace transform exact solution	Stratification, diffusion, magnetic field	Stratification reduces velocity but improves heat and mass transfer efficiency
Aroloye et al., (2024) [25]	MHD flow with chemical reaction and radiation	Runge–Kutta shooting method (Maple)	Schmidt no., Soret no., permeability, radiation	Parameters significantly affect velocity, temperature, concentration
Islam et al., (2024) [26]	Casson fluid free convection through porous medium	Finite Difference Method	Magnetic parameter, skin friction, heat & mass transfer	Magnetic parameter increases plate temperature

Sudarmozhi et al., (2024) [27]	Maxwell viscoelastic fluid on porous plate	bvp4c MATLAB solver	Rayleigh no., radiation, porous parameter	Velocity increases with Rayleigh number; temperature rises with radiation
Das et al., (2024) [28]	Oscillating vertical plate in porous medium	Laplace transform analytical solution	Magnetic, Grashof, radiation, permeability	Radiation and magnetic parameters significantly affect heat transfer
Prakash et al., (2024) [29]	MHD Casson fluid in rotating porous medium	Analytical Laplace transform	Radiation, heat generation, Prandtl, Schmidt	Heat generation retards velocity & temperature
Reddy et al., (2023) [30]	Water-based nanofluid in porous medium	Finite Element Method	Radiation, magnetic parameter	Radiation increases velocity & temperature; magnetic field decreases velocity
Hasanuzzaman et al., (2023) [31]	Radiative MHD flow over porous sheet	Finite Difference Method	Eckert, Prandtl, Schmidt numbers	Eckert increases velocity; Prandtl increases heat transfer rate
Prabhakar et al., (2023) [32]	Inclined permeable plate with chemical reaction	DuFort–Frankel finite difference	Radiation, inclination, Thermodiffusion	Magnetic field decreases velocity; radiation increases Nusselt number
Uddin et al., (2023) [33]	Boundary layer free convection over permeable plate	Explicit finite difference	Radiation, buoyancy force	Radiation decreases temperature within boundary layer
Sarma et al., (2022) [34]	Radiative chemically reacting MHD flow	Laplace transform analytical solution	Soret number, radiation	Radiation increases Nusselt number but reduces Soret effect
Poddar et al., (2022) [35]	Rotating radiative MHD flow with Hall current	Explicit Finite Difference	Magnetic parameter, porosity, radiation	Stability and convergence verified; parameters

				influence flow behavior

3. RESEARCH OBJECTIVES

- To formulate the governing equations for unsteady magnetohydrodynamic free convection flow of a Casson fluid past an infinite vertical plate with coupled heat and mass transfer.
- To study the effects of thermal radiation and internal heat generation/absorption on the velocity, temperature, and concentration fields.
- To obtain numerical solutions of the resulting nonlinear coupled partial differential equations using the Crank–Nicolson finite difference method.
- To analyse the influence of key physical parameters on the flow, thermal, and concentration characteristics through graphical results.
- To evaluate the skin-friction coefficient, rate of heat transfer, and rate of mass transfer at the plate in nondimensional form.

4. RESEARCH METHODOLOGY

4.1 Physical Model and Flow Assumptions

The present study examines an unsteady, two-dimensional, laminar, incompressible magnetohydrodynamic (MHD) free-convection flow of a Casson fluid past an infinite vertical flat plate with coupled heat and mass transfer effects. The flow is assumed to be initially quiescent and subsequently driven by thermal and solutal buoyancy forces arising from temperature and concentration differences between the plate surface and the ambient fluid. A Cartesian coordinate system is adopted in which the x-axis is aligned vertically upward along the plate, while the y-axis is taken normal to the plate surface into the fluid region. Since the plate is considered infinite in the x-direction, all physical variables depend only on the transverse coordinate y and time t, there by reducing the problem to a one-dimensional transient boundary-layer formulation. The physical configuration of the present problem and the coordinate system adopted for analysis are illustrated in Figure 1.

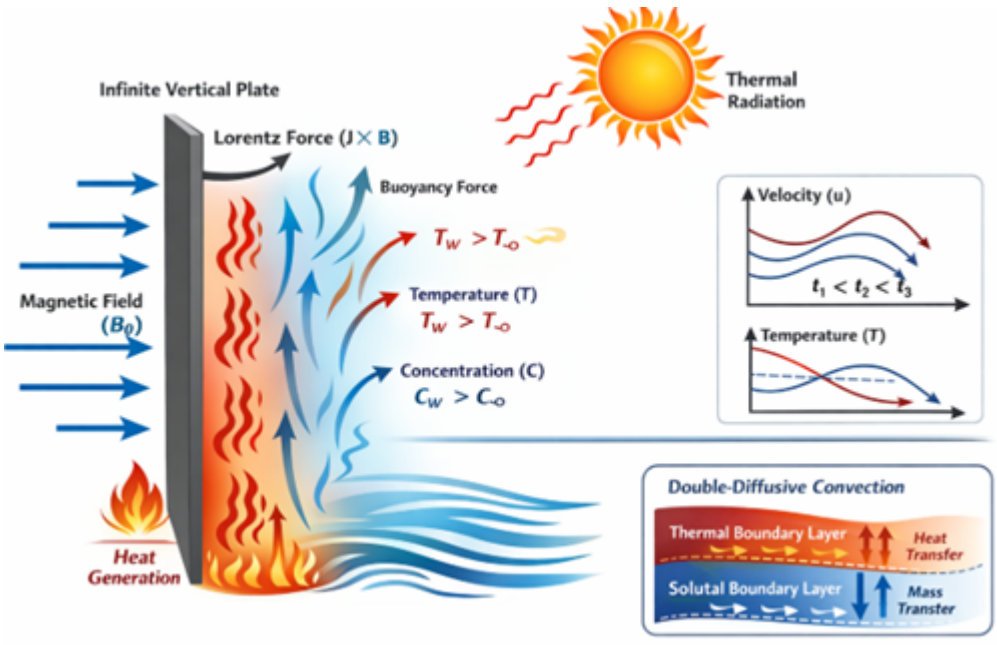

Figure 1: Velocity, Temperature, and Concentration profiles in unsteady MHD flow

A uniform transverse magnetic field of constant strength B_0 is applied perpendicular to the plate. The fluid is electrically conducting, and the magnetic Reynolds number is assumed to be sufficiently small such that the induced magnetic field is negligible in comparison with the applied magnetic field. Consequently, the Lorentz force arising from the interaction between the magnetic field and the fluid motion is incorporated in the momentum equation, while Hall effects and Joule heating are neglected. The fluid is assumed to be optically thick, allowing the radiative heat flux to be modeled using the Rosseland diffusion approximation. Internal heat generation or absorption within the fluid is considered in the energy balance to account for volumetric heat source or sink effects. Mass diffusion is incorporated through Fick's law in the species concentration equation.

The working fluid is modeled as a Casson non-Newtonian fluid to capture yield-stress behavior and shear-thinning characteristics. The Casson parameter represents the ratio of yield stress to viscous stress and modifies the effective viscosity in the momentum equation. All thermo physical properties of the fluid are assumed constant except for density variations in the buoyancy terms. These density variations are treated using the Boussinesq approximation, whereby density differences are considered only in the gravitational body-force terms responsible for thermal and solutal convection. Under these assumptions, the governing equations reduce to a coupled system of transient nonlinear partial differential equations representing conservation of momentum, energy, and species concentration within the boundary layer region.

4.2 Governing Equations

Under the boundary-layer approximations for an incompressible electrically conducting fluid, the conservation equations of mass, momentum, energy, and species concentration govern the flow. The buoyancy forces arise due to temperature and concentration differences and are incorporated using the Boussinesq approximation. The non-Newtonian behavior of the Casson fluid modifies the effective viscosity in the momentum equation through the Casson parameter β, while the applied magnetic field introduces a resistive Lorentz force opposing the fluid motion.

- ***Continuity Equation***

For a one-dimensional transient boundary-layer flow, the continuity equation reduces to

$$\frac{\partial v}{\partial y} = 0 \qquad (1)$$

which implies that the normal velocity component remains constant across the boundary layer.

- ***Momentum Equation***

The momentum balance includes viscous diffusion, buoyancy forces due to thermal and solutal gradients, and magnetic damping:

$$\frac{\partial u}{\partial t} = \nu\,,\left(1+\frac{1}{\beta}\right)\frac{\partial^2 u}{\partial y^2} + g\beta_T(T-T_\infty) + g\beta_C(C-C_\infty) - \frac{\sigma B_0^2}{\rho}u \qquad (2)$$

The first term on the right represents modified viscous diffusion for a Casson fluid, the second and third terms correspond to thermal and solutal buoyancy forces, and the last term

denotes the Lorentz force generated by the interaction of the magnetic field with the electrically conducting fluid.

- ***Energy Equation***

The energy equation accounts for thermal conduction, radiative heat flux, and volumetric heat generation/absorption:

$$\frac{\partial T}{\partial t} = \alpha \frac{\partial^2 T}{\partial y^2} - \frac{1}{\rho c_p}\frac{\partial q_r}{\partial y} + \frac{Q_0}{\rho c_p}(T - T_\infty) \qquad (3)$$

The second term represents divergence of radiative heat flux, while the third term models internal heat generation ($Q_0 > 0$) or absorption ($Q_0 < 0$).

- ***Concentration Equation***

Mass transport within the boundary layer is governed by Fick's diffusion law:

$$\frac{\partial C}{\partial t} = D\frac{\partial^2 C}{\partial y^2} \qquad (4)$$

which describes species diffusion due to concentration gradients.

- ***Physical Variables***

u– velocity component along the plate$T$– temperature

C– concentration

β– Casson fluid parameter

ν– kinematic viscosity

α– thermal diffusivity

D– mass diffusivity

These coupled nonlinear partial differential equations describe the transient momentum, thermal, and concentration boundary-layer development under the combined influence of magnetic field, buoyancy, radiation, and heat generation effects.

4.3 Thermal Radiation Modeling

Thermal radiation effects are incorporated into the energy equation using the Rosseland diffusion approximation, which is appropriate for optically thick fluids where radiative heat transfer occurs predominantly by diffusion rather than wave propagation. Under this approximation, the radiative heat flux is expressed as

$$q_r = -\frac{4\sigma^*}{3k^*}\frac{\partial T^4}{\partial y} \qquad (5)$$

where σ^* is the Stefan–Boltzmann constant and k^* is the mean absorption coefficient of the medium. This formulation assumes that the radiation intensity is nearly isotropic and that temperature gradients within the boundary layer are sufficiently small.

To linearize the nonlinear term T^4, a Taylor series expansion about the ambient temperature T_∞ is performed. Neglecting higher-order terms yields

$$T^4 \approx 4T_\infty^3 T - 3T_\infty^4$$

Substituting this relation into Eq. (5) gives

$$q_r = -\frac{16\sigma^* T_\infty^3}{3k^*}\frac{\partial T}{\partial y}$$

Replacing the radiative heat flux in the dimensional energy equation results in the modified energy balance

$$\frac{\partial T}{\partial t} = \left(\alpha + \frac{16\sigma^* T_\infty^3}{3\rho c_p k^*}\right)\frac{\partial^2 T}{\partial y^2} + \frac{Q_0}{\rho c_p}(T - T_\infty) \qquad (6)$$

The radiation term effectively enhances thermal diffusivity, indicating that thermal radiation increases the rate of heat transport within the boundary layer.

4.4 Non-Dimensionalisation

To generalize the governing equations and identify the controlling physical parameters, suitable dimensionless variables are introduced using a characteristic velocity $U_0$and the viscous length scale ν/U_0:

$$y^* = \frac{yU_0}{\nu}, t^* = \frac{tU_0^2}{\nu}, U = \frac{u}{U_0}, \theta = \frac{T - T_\infty}{T_w - T_\infty}, \phi = \frac{C - C_\infty}{C_w - C_\infty}$$

After substituting these variables into the dimensional governing equations and simplifying, the following nondimensional system is obtained.

- ***Momentum Equation***

$$\frac{\partial U}{\partial t} = \left(1 + \frac{1}{\beta}\right)\frac{\partial^2 U}{\partial y^2} + Gr\,\theta + Gc\,\phi - MU \qquad (7)$$

This equation shows the competition between viscous diffusion, buoyancy forces, and magnetic damping (Lorentz force).

- ***Energy Equation***

$$\frac{\partial \theta}{\partial t} = \frac{1}{Pr}\left(1 + \frac{4R}{3}\right)\frac{\partial^2 \theta}{\partial y^2} + Q\,\theta \qquad (8)$$

The radiation term modifies the effective thermal diffusivity, indicating enhancement of heat transport due to thermal radiation.

- ***Concentration Equation***

$$\frac{\partial \phi}{\partial t} = \frac{1}{Sc}\frac{\partial^2 \phi}{\partial y^2} \qquad (9)$$

This equation describes mass diffusion within the boundary layer.

- ***Dimensionless Parameters***

$$Gr = \frac{g\beta_T(T_w - T_\infty)\nu}{U_0^3} \text{(thermal Grashof number)}$$

$$Gc = \frac{g\beta_C(C_w - C_\infty)\nu}{U_0^3} \text{(solutal Grashof number)}$$

$$M = \frac{\sigma B_0^2 \nu}{\rho U_0^2} \text{(magnetic parameter)}$$

$$Pr = \frac{\nu}{\alpha} \text{(Prandtl number)}$$

$$Sc = \frac{\nu}{D} \text{(Schmidt number)}$$

$$R = \frac{4\sigma^* T_\infty^3}{kk^*} \text{(radiation parameter)}$$

$$Q = \frac{Q_0 \nu}{\rho c_p U_0^2} \text{(heat generation/absorption parameter)}$$

The nondimensional formulation reduces the number of independent variables and reveals the relative importance of buoyancy, viscous, magnetic, radiative, and diffusive transport mechanisms governing the transient MHD convection process.

4.5 Initial and Boundary Conditions

The nondimensional governing equations are solved subject to physically realistic initial and boundary conditions corresponding to an impulsively heated and concentrated vertical plate.

- ***Initial Condition ($t \leq 0$)***

Initially, the fluid and plate are assumed to be at rest and in thermal and concentration equilibrium with the ambient fluid. Therefore,

$$U = 0, \theta = 0, \phi = 0 \text{ for all } y \qquad (10)$$

- ***Boundary Condition at the Plate Surface ($y = 0$, $t > 0$)***

At time $t > 0$, the plate temperature and concentration are suddenly raised to constant values $T_w$and C_w, while the plate remains stationary. Hence,

$$U = 0, \theta = 1, \phi = 1 \qquad (11)$$

This represents a classical thermal and solutal boundary-layer development over an isothermal vertical plate.

- ***Free Stream Condition ($y \to \infty$)***

Far away from the plate, the fluid remains unaffected by the surface heating and mass diffusion:

$$U \to 0, \theta \to 0, \phi \to 0 \qquad (12)$$

4.6 Numerical Solution Procedure

The coupled transient nonlinear partial differential equations (7)–(9), together with the boundary conditions (10)–(12), are solved numerically using the Crank–Nicolson implicit finite difference method. This scheme is adopted due to its second-order accuracy in both time and space and unconditional stability for diffusion-dominated transport problems.

Time derivatives are discretize using the trapezoidal formulation, while spatial derivatives are approximated by central difference approximations on a uniform grid. The discretization process transforms the governing equations into a set of linear algebraic equations at each time level, forming a tri-diagonal matrix system. The resulting tri-diagonal system is efficiently solved using the Thomas algorithm. Iterations are performed at each time step until convergence is achieved with a tolerance of 10^{-6}. Grid independence and time-step sensitivity are verified to ensure numerical accuracy and stability of the solution.

4.7 Engineering Quantities of Interest

To evaluate the physical characteristics of the flow and transport processes, the following engineering parameters are computed at the plate surface.

- ***Skin-Friction Coefficient***

The wall shear stress, which measures the resistive drag exerted by the fluid on the plate, is expressed in nondimensional form as

$$C_f = \left(1+\frac{1}{\beta}\right)\frac{\partial U}{\partial y}\,|_{y=0} \qquad (13)$$

- ***Nusselt Number***

The rate of heat transfer from the plate to the fluid is represented by the local Nusselt number

$$Nu = -\frac{\partial \theta}{\partial y}\,|_{y=0} \qquad (14)$$

- ***Sherwood Number***

The rate of mass transfer at the surface is quantified by the Sherwood number

$$Sh = -\frac{\partial \phi}{\partial y}\,|_{y=0} \qquad (15)$$

These parameters provide a direct measure of momentum, heat, and mass transfer characteristics of the transient MHD Casson fluid flow under the influence of thermal radiation and internal heat generation.

5. Result and Analysis

The velocity profile shown in figure 2 is a typical boundary-layer behavior with a single peak. At the plate surface ($y = 0$), the velocity U is zero due to the no-slip condition. The velocity increases rapidly between y and U maximum value of approximately $U \approx 2.3$ to 2.4 occurs at y values between 1.3 and 1.5. The peak point shows that buoyancy forces operate with greater strength near the wall. The velocity starts to drop when the two factors viscous damping and magnetic damping reach their peak effects. The velocity at y approximately 3 decreases to $U \approx 1.5$ and then maintains a further decrease until it reaches $U \approx 0.5$ at y approximately 5. The velocity approaches zero as y exceeds 8 which meets the free-stream boundary condition. The curve shows transient MHD free convection flow through its smooth continuous decay of flow.

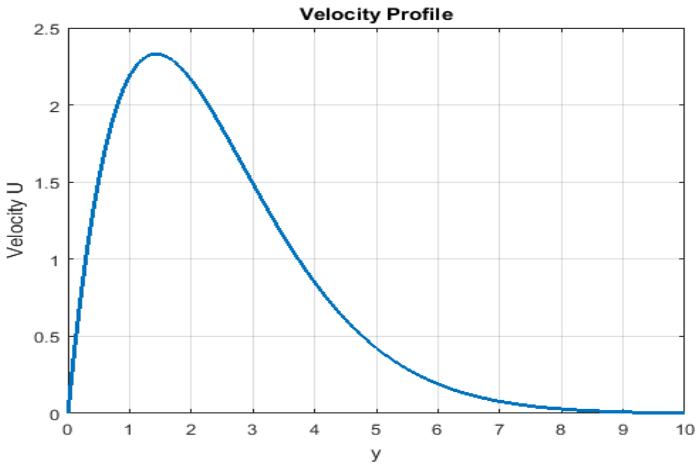

Figure2: Velocity profile for unsteady MHD free convection flow of a Casson fluid

The concentration profile at figure 3 shows an uninterrupted decline which extends from the plate surface to the entire fluid domain. The wall at (y = 0) shows its highest concentration level because $\phi = 1$ which meets the required surface concentration standard. The

concentration patterns show rapid decline which results from molecular diffusion when observers move away from the plate. The concentration at approximately y ≈ 1 reaches a value of ϕ ≈ 0.6 and then it decreases to ϕ ≈ 0.28again at y ≈ 2.

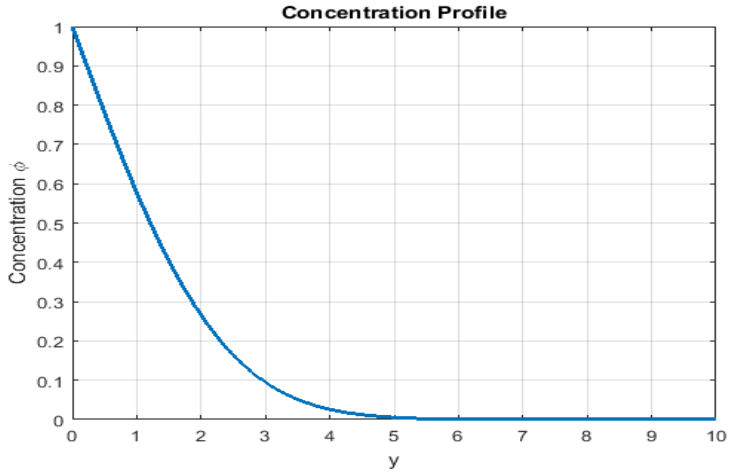

Figure 3: Concentration distribution for unsteady MHD Casson fluid flow

The value reaches a near drop to $\phi \approx 0.1$ at approximately $y \approx 3$. The concentration level drops to extremely low values which exist below 0.03┤ and yet it maintains an asymptotic approach to zero which starts at $y \geq 5$ and this shows the location of the concentration boundary layer limit. The smooth exponential-type decay shows that diffusive mass transport dominates the transient convection–diffusion process.

The temperature profile in figure 4 shows a smooth monotonic decay from the heated plate into the ambient fluid. At the wall ($y = 0$), the dimensionless temperature is maximum, $\theta = 1$, satisfying the imposed thermal boundary condition. As y increases, the temperature decreases gradually due to thermal diffusion.

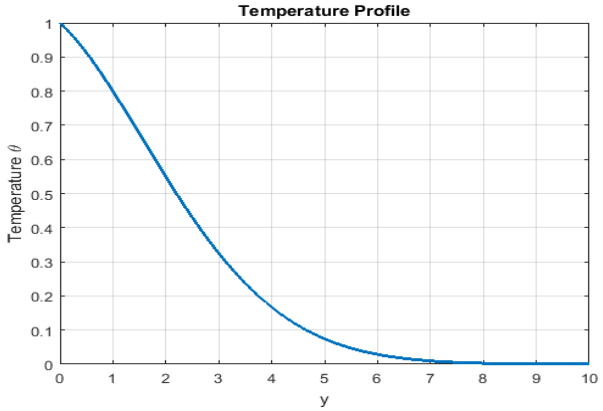

Figure 4: Temperature distribution for unsteady MHD Casson fluid flow with thermal radiation

At approximately $y \approx 1$, θ reduces to about 0.8, and at $y \approx 2$ it falls to nearly 0.55. Around $y \approx 3$, the temperature further declines to $\theta \approx 0.32$, indicating significant heat dissipation within the thermal boundary layer. By $y \approx 5$, θ becomes nearly 0.08, and beyond $y \approx 7$ it approaches zero asymptotically, satisfying the free-stream condition. The continuous exponential-type decay reflects dominant conductive and radiative heat transfer effects in the transient boundary-layer flow.

The graph in figure 5 shows the effect of the magnetic parameter Mon the velocity distribution in the boundary layer. In all the cases, when the plate is at a distance, $y = 0$, the velocity is zero as a result of the no-slip condition, then it accelerates, reaches its highest point, and then decreases asymptotically with an increase in the plate distance, y. In the case of $M = 0.5$, velocity has the maximum peak of $U = 1.5$ relates to $y = 1.5$. As the magnetic parameter M approaches 1, the peak velocity reduces to almost $U = 2.3$ at almost the same point. In the case of a more intense magnetic field $M = 2$, the maximum velocity is reduced to a lower value of about $U = 1.7$. At a value of y larger than $y = 4$ all the profiles drop substantially and the velocity reaches near 0 at, $y = 8$. The increasing deceleration of velocity with increasing M demonstrates the dragging force -Lorentz force that inhibits fluid motion and dilutes the momentum boundary layer.

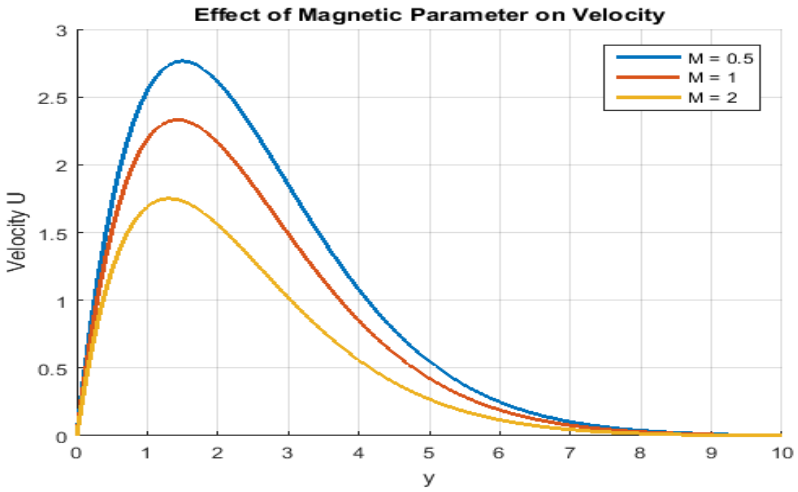

Figure 5: Effect of magnetic parameter (M) on the velocity profile of Casson fluid flow

The graph in figure 6 shows how the Casson parameter β affects the velocity distribution that occurs in the boundary layer. The velocity at the wall ($y = 0$) starts from U = 0 and then increases rapidly to reach its highest point before it gradually decreases to zero value as y increases.

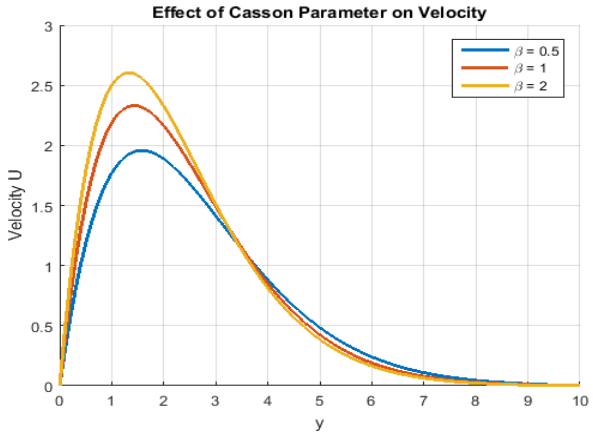

Figure 6: Effect of Casson parameter (β) on the velocity profile

The peak velocity for $\beta = 0.5$ occurs at approximately $U \approx 1.95$ at $y \approx 1.6$. The maximum velocity increases to about $U \approx 2.3$ when β reaches 1 and occurs at almost the same location. The peak velocity for $\beta = 2$ reaches approximately $U \approx 2.6$. The profiles start to merge after $y \approx 3.5$ and by $y \approx 8 - 9$ all β values show that velocity reaches zero.

The numerical trend shows that higher β values lead to increased fluid velocity and greater momentum boundary layer thickness because Casson fluid exhibits reduced yield stress effects and exhibits weaker resistance to flow.

The figure 7 demonstrate how the temperature distribution caused by R on the radiation parameter, changes in the thermal boundary layer. At the plate surface ($y = 0$), the non-dimensional temperature is $\theta = 1$ in all the cases. The farther the plate the lower the temperature which slowly tends towards zero. In the case of $R = 0.5$, the temperature decreases with a very low rate, with the approximate temperature of 0.25 at $y = 3$ and almost zero at $y = 6$. At $R = 1$, the decay is slower, with 0 with an approximate value of 0.35 at $y = 3$ and it approaches zero at approximately $y = 7$. At $R = 2$ temperature is still higher along the boundary layer $09^{th} = 0.48$ at $y = 3$ and the effect can still be seen further down to y = "8 - 9". Therefore, a greater amount of thermal radiation augments heat diffusion, enlarges a thermal boundary layer, and sustains greater fluid temperature as distant as the plate.

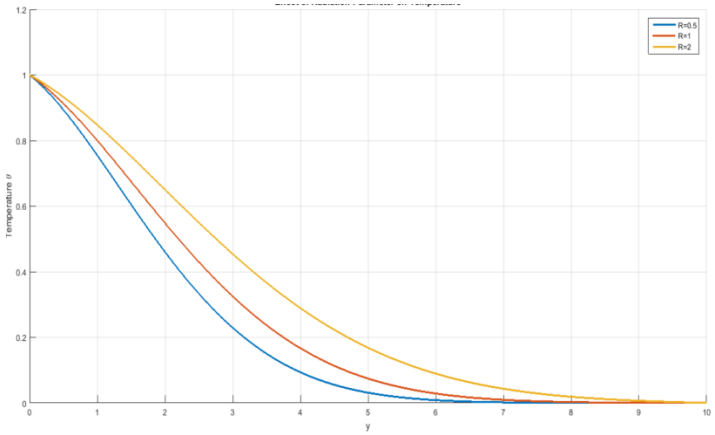

Figure 7: Effect of Radiation Parameter (R) on Temperature Profile

Figure 8 displays how dimensionless temperature θ changes with the transverse coordinate y at three different heat generation levels Q. The temperature decreases monotonically from the wall toward the free stream region for all cases, indicating thermal diffusion away from the surface. The temperature distribution across the boundary layer shows significant increase because of higher Q values. The thermal boundary layer reaches its minimum thickness at $Q = 0$ because the temperature decreases at an extreme rate.

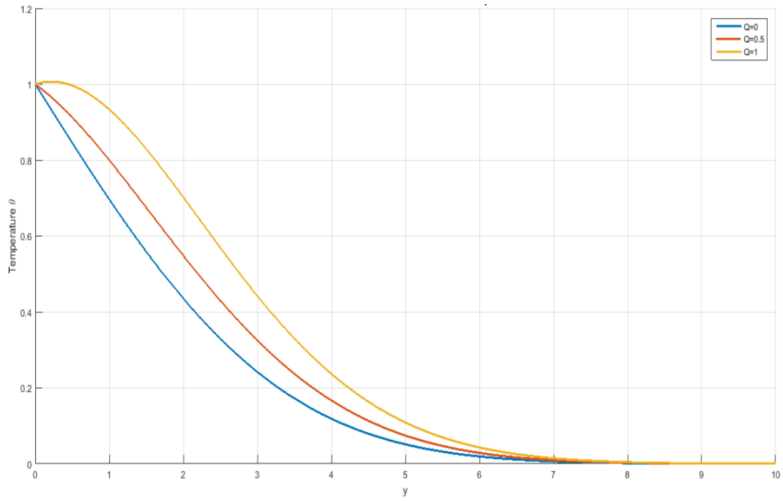

Figure 8: Effect of Heat Generation Parameter (Q) on Temperature Profile

The decay at $Q = 0.5$ shows a moderate thermal thickening pattern because it decreases at a slower rate. The temperature at $Q = 1$ remains at its highest level because it decreases at the slowest rate, which shows how strong internal heat sources provide extra energy to the fluid while increasing thermal boundary layer thickness. The results show that increased heat generation results in higher fluid temperatures and extended cooling times, which confirms that internal heat production leads to greater thermal energy storage within the flow field.

The graph in figure 9 of velocity profile U versus transverse coordinate y shows the velocity profile of the three Grashof numbers: $Gr = 2,5,10$. In each case, the velocity is zero at the wall ($y = 0$), attains a maximum then decreases slowly towards zero as y is nearer to 10. In the case of $Gr = 2$, the maximum velocity is about $U = 1.6$ at $y = 1.5$. The speed becomes 0.5 at $y = 4$ and almost zero at $y = 7$. In the case of $Gr = 5$ maximum velocity rises to approximately $U = 2.6$ around $y = 1.5$ and decays more slowly than in the case of $Gr = 2$. In the case of $Gr = 10$, the maximum value is about $U_{max} = 4.4$ $y_{max} = 1.5$ and the boundary layer is thicker. Therefore, an increment in Gr considerably improves the magnitude of velocity and momentum boundary layer thickness as a result of increment in the magnitude of buoyancy forces.

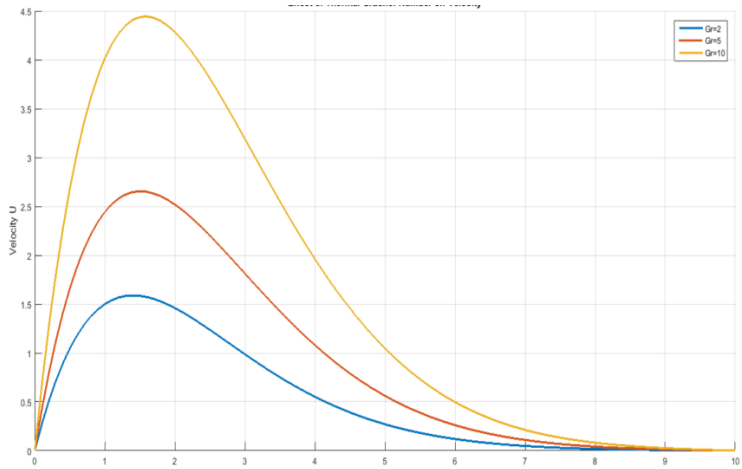

Figure 9: Effect of Thermal Grashof Number (Gr) on Velocity Profile

The figure 10 shows the concentration profile ϕ versus the transverse coordinate y for three Schmidt numbers: $Sc = 0.22, 0.62, 1$. At the beginning of all experiments, concentration starts at ϕ=1 which exists at the surface ($y = 0$) and the level of concentration decreases in a continuous manner until it reaches zero at higher y values.

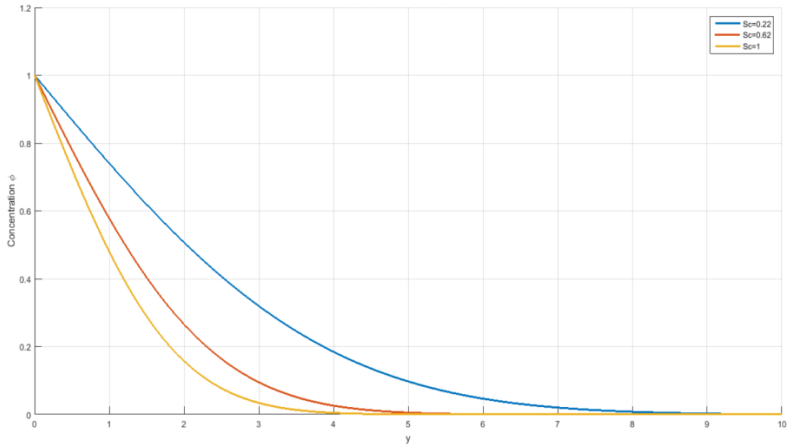

Figure 10: Effect of Schmidt Number (Sc) on Concentration Profile

For $Sc = 0.22$, concentration decreases gradually, reaching $\phi \approx 0.5$ at $y \approx 1.8, \phi \approx 0.2$ at y≈3.5, and approaching zero near $y \approx 9$. The results show that the system has a wide concentration boundary layer. For Sc=0.62, the decay is faster: $\phi \approx 0.3$at $y \approx 2$, and nearly zero by $y \approx 5$. For $Sc = 1$, concentration drops most rapidly, becoming almost zero around $y \approx 4$. The process of increasing Sc causes a decrease in concentration levels which results in a thinner concentration boundary layer because of decreased mass diffusivity.

In the figure 11 the changing behavior of the coefficient of skin-friction, C_f, as a function of a controlling parameter (rising along the horizontal axis between 0.5 and 2.5) is depicted. We can see the evident decreasing trend as the curve approaches the skin friction at its maximum at approximately C_f = 14.5 when the parameter is 0.5 and goes down to approximately C_f = 9.9 when the parameter is 2.5. The cut is nearly linear which means that there is a constant decrease of the wall shear stress due to the parameter. Physically, this action implies the momentum boundary layer increases in thickness and therefore reduces the velocity gradient by the wall and thus the shear force acting on the surface is decreased. The decrease is stronger between 0.5 and 1.5 and then becomes slightly more even, which suggests the decrease in sensitivity at large values. In general, the larger the governing parameter, the lower the fluid resistance around the plate and the lesser the frictional drag as well as the flow regime is more stable.

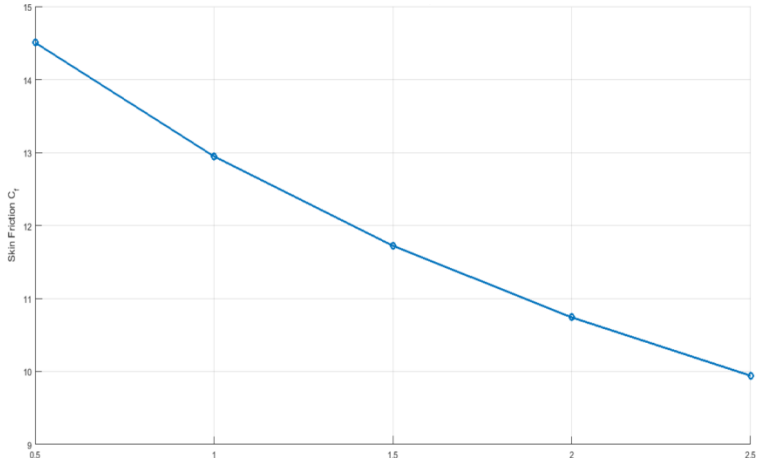

Figure 11: Variation of Skin-Friction Coefficient (Cf) with Magnetic Parameter (M)

The graph in figure 12 represents how the Nusselt number (Nu) changes with the parameter of radiation (R) between 0.5 0.5 0.5 -1 and 2 2 -1. In numerical the Nusselt number at $R = 0.5$ is such that, it is close to the minimum value of the heat transfer with an approximate value of -0.055. When R increases to 1.0, Nu increases to approximately -0.0495 indicating a gain of approximately 0.0055. As R is further increased to 1.5, Nu is then closer to -0.045 indicating an increase of about 0.0045 more units. At $R = 2.0$, Nusselt number equals about −0.042, the maximum value. In general, Nusselt number rises by almost 0.013 units when the R changes in the range 0.5 to 2.0. The values are negative over the entire range, although, it reduces in magnitude steadily, indicating that the greater the values of the radiation parameters the higher the rate of heat transfer at the surface in an almost linear and monotonic way within the range of the research.

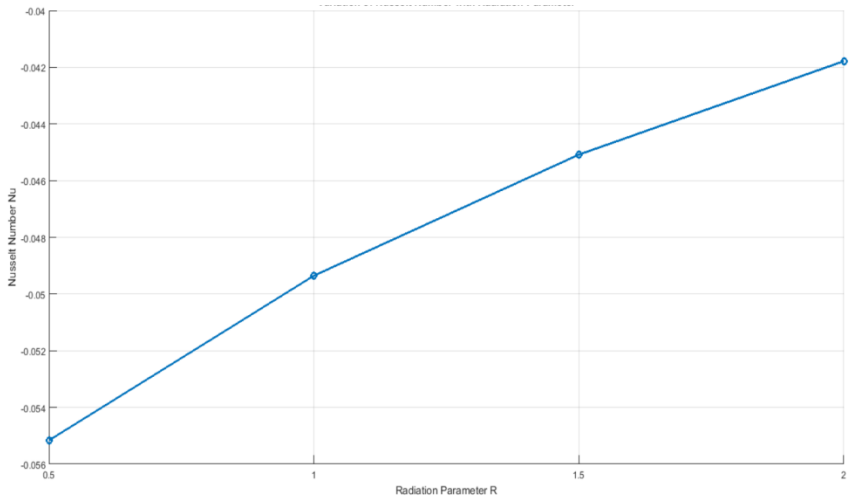

Figure 12: Variation of Nusselt Number (Nu) with Radiation Parameter (R)

Table 2 presents the physical and numerical parameters employed in the computational analysis. The Casson parameter β (0.5–2) characterizes the non-Newtonian behavior of the fluid, while the magnetic parameter M (0.5–2.5) represents the applied magnetic field strength. Thermal buoyancy is controlled by the thermal Grashof number Gr (2, 5, 10), whereas the solutal Grashof number Gc is fixed at 5.

Table 2: Physical and Numerical Parameters Used in Computation

Parameter	**Symbol**	**Value(s) Used**	**Description**
Casson parameter	β	0.5, 1, 2	Non-Newtonian fluid parameter
Magnetic parameter	M	0.5, 1, 1.5, 2, 2.5	Strength of the applied magnetic field
Thermal Grashof number	Gr	2, 5, 10	Thermal buoyancy parameter
Solutal Grashof number	Gc	5	Solutal buoyancy parameter (fixed)
Prandtl number	Pr	0.71	Ratio of momentum to thermal diffusivity
Schmidt number	Sc	0.22, 0.62, 1	Ratio of momentum to mass diffusivity
Radiation parameter	R	0.5, 1, 1.5, 2	Thermal radiation effect
Heat generation parameter	Q	0, 0.5, 1	Internal heat source/sink
Maximum transverse distance	y_{max}	10	Computational domain size
Number of grid points	Ny	101	Spatial discretization
Number of time steps	N_t	200	Temporal discretization

The Prandtl number $Pr = 0.71$ indicates air-type fluid properties. Mass diffusion effects are examined using Schmidt number Sc (0.22, 0.62, 1). Radiation parameter R (0.5–2) and heat generation parameter Q (0–1) model thermal energy effects. The computational

domain extends to y_{max} = 10 with 101 grid points and 200-time steps ensuring numerical accuracy.

6. CONCLUSION AND FUTURE SCOPE

In the current study, the joint role of thermal radiation, internal heat, magnetic field, and buoyancy forces in free convection unsteady MHD flow in the Casson fluid past an infinite vertical plate with heat and mass exchange were considered. The Crank Nicolson finite difference approach was able to provide stable accurate numerical solutions in 101 grid points and 200-time steps. Findings have shown that the higher the radiation parameter is, that is, when $R = 0.5$ moves to 2.0, the higher the Nusselt number becomes in the range of $N = -0.055$ to $N = -0.042$, which represents a better heat transfer. As the thermal Grashof number went up, the maximum velocity rose considerably, 1.6 to 4.4, which validates the becoming even stronger of the buoyancy effects. On the other hand, an increase in magnetic parameter decreased velocity and skin-friction coefficient by about 14.5 to 9.9 and is an example of Lorentz force damping. Concentration increases in the Schmidt number, by increasing Schmidt number between 0.22 and 1 increased markedly thickness of concentration. In general, the production of radiation and heat caused a thickening of the thermal boundary layer, whereas the magnetic effects stabilized the flow.

In the future, the model has the capacity of further expansion to incorporate variable fluid properties, Joule heating, Hall current, and slip boundary conditions in a more realistic depiction of industrial processes. Effects of nanofluids, hybrid nanoparticles, or porous media can be used to improve thermal performance predictions. Computational efficiency could be enhanced by using the more sophisticated numerical methods like spectral methods or machine learning-aid solvers. In addition, practical applicability in aerospace cooling, nuclear reactors and advanced energy systems would be enhanced by experimental validation, three-dimensional transient simulations.

Nomenclature

Symbol	Description	Unit
(u)	Velocity component along the vertical plate	m/s
(y)	Transverse coordinate normal to the plate	m
(t)	Time	s
(T)	Fluid temperature	K
(C)	Species concentration	kg/m³
(T∞)	Ambient fluid temperature	K
(C∞)	Ambient concentration	kg/m³
(T_w)	Plate surface temperature	K
(C_w)	Plate surface concentration	kg/m³
(ν)	Kinematic viscosity of fluid	m²/s
(α)	Thermal diffusivity	m²/s
(D)	Mass diffusivity	m²/s
(β)	Casson fluid parameter	–
(B_0)	Applied magnetic field strength	Tesla
(σ)	Electrical conductivity of fluid	S/m
(g)	Acceleration due to gravity	m/s²

(β_T)	Thermal expansion coefficient	1/K
(β_C)	Concentration expansion coefficient	1/(kg/m³)
(k)	Thermal conductivity	W/mK
(q_r)	Radiative heat flux	W/m²
(σ^*)	Stefan–Boltzmann constant	W/m²K⁴
(k*)	Mean absorption coefficient	m^{-1}
(Q)	Heat generation parameter	–
(M)	Magnetic parameter	–
(Gr)	Thermal Grashof number	–
(Gc)	Solutal Grashof number	–
(Pr)	Prandtl number	–
(Sc)	Schmidt number	–
(R)	Radiation parameter	–
(Nu)	Nusselt number (heat transfer rate)	–
(Sh)	Sherwood number (mass transfer rate)	–
(C_f)	Skin friction coefficient	–
(θ)	Dimensionless temperature	–
(ϕ)	Dimensionless concentration	–

7. REFERENCES

[1] Kabeel, A. E., Emad MS El-Said, and S. A. Dafea. "A review of magnetic field effects on flow and heat transfer in liquids: present status and future potential for studies and applications." Renewable and Sustainable Energy Reviews 45 (2015): 830-837.

[2] Cao, Bing-Yang, Jun Sun, Min Chen, and Zeng-Yuan Guo. "Molecular momentum transport at fluid-solid interfaces in MEMS/NEMS: a review." International journal of molecular sciences 10, no. 11 (2009): 4638-4706.

[3] Ali, Farhad, Muhammad Bilal, Madeha Gohar, Ilyas Khan, Nadeem Ahmad Sheikh, and KottakkaranSooppy Nisar. "A report on fluctuating free convection flow of heat absorbing viscoelastic dusty fluid past in a horizontal channel with MHD effect." Scientific Reports 10, no. 1 (2020): 8523.

[4] To, W. M., and J. A. C. Humphrey. "Numerical simulation of buoyant, turbulent flow—I. Free convection along a heated, vertical, flat plate." International journal of heat and mass transfer 29, no. 4 (1986): 573-592.

[5] Ahmed, Sahin, Joaquín Zueco, and Luis M. López-González. "Effects of chemical reaction, heat and mass transfer and viscous dissipation over a MHD flow in a vertical porous wall using perturbation method." International Journal of Heat and Mass Transfer 104 (2017): 409-418.

[6] Breuer, Kenneth S., Jinil Park, and Charles Henoch. "Actuation and control of a turbulent channel flow using Lorentz forces." Physics of Fluids 16, no. 4 (2004): 897-907.

[7] Nobrega, Glauco, Beatriz Cardoso, Reinaldo Souza, José Pereira, Pedro Pontes, Susana O. Catarino, Diana Pinho, Rui Lima, and Ana Moita. "A review of novel heat transfer materials and fluids for aerospace applications." Aerospace 11, no. 4 (2024): 275.

[8] Solomon, T. H., and Jerry P. Gollub. "Thermal boundary layers and heat flux in turbulent convection: the role of recirculating flows." Physical Review A 43, no. 12 (1991): 6683.

[9] Seddeek, M. A. "Finite-element method for the effects of chemical reaction, variable viscosity, thermophoresis and heat generation/absorption on a boundary-layer hydromagnetic flow with heat and mass transfer over a heat surface." Acta Mechanica 177, no. 1 (2005): 1-18.

[10] Salimipour, Erfan. "Thermal buoyancy effects on the flow field and heat transfer of a rotating cylinder: A numerical study." International Journal of Thermal Sciences 155 (2020): 106453.

[11] Sedki, Ahmed M., S. M. Abo-Dahab, J. Bouslimi, and K. H. Mahmoud. "Thermal radiation effect on unsteady mixed convection boundary layer flow and heat transfer of nanofluid over permeable stretching surface through porous medium in the presence of heat generation." Science Progress 104, no. 3 (2021): 00368504211042261.

[12] Norton, Tomás, Brijesh Tiwari, and Da-Wen Sun. "Computational fluid dynamics in the design and analysis of thermal processes: a review of recent advances." Critical reviews in food science and nutrition 53, no. 3 (2013): 251-275.

[13] Mojtabi, Abdelkader, and Marie-Catherine Charrier-Mojtabi. "Double-diffusive convection in porous media." In Handbook of Porous media, pp. 287-338. CRC Press, 2005.

[14] García-Ybarra, Pedro L., and Jose L. Castillo. "Mass transfer dominated by thermal diffusion in laminar boundary layers." Journal of Fluid Mechanics 336 (1997): 379-409.

[15] Buschmann, M. H., P. Dieterich, N. A. Adams, and H-J. Schnittler. "Analysis of flow in a cone-and-plate apparatus with respect to spatial and temporal effects on endothelial cells." Biotechnology and bioengineering 89, no. 5 (2005): 493-502.

[16] García García, F. Javier. "Transient discharge of a pressurised incompressible fluid through a pipe and analytical solution for unsteady turbulent pipe flow." (2017).

[17] Kuntz, David, and Peter Grathwohl. "Comparison of steady-state and transient flow conditions on reactive transport of contaminants in the vadose soil zone." Journal of hydrology 369, no. 3-4 (2009): 225-233.

[18] Sheiso, Desta Sodano, and Saket Apparao Kuchibhotla. "Comparison of the Coupled Solution of the Species, Mass, Momentum, and Energy Conservation Equations by Unstructured FVM, FDM, and FEM." Int. J. Appl. Math. Theor. Phys. 8 (2022): 52-57.

[19] Oane, Mihai, Muhammad Arif Mahmood, and Andrei C. Popescu. "A state-of-the-art review on integral transform technique in laser–material interaction: Fourier and non-Fourier heat equations." Materials 14, no. 16 (2021): 4733.

[20] Zamri, Nur Hazwani, Abdul Rahman Mohd Kasim, Mohd Haziezan Hassan, Tijjani Lawal Hassan, Syazwani Mohd Zokri, Nur Syamilah Arifin, and Adeosun Adeshina Taofeeq. "Theoretical Analysis of Two-Phase Mixed Convection Flow: Effects of Fluid-particle Interaction and Mass Concentration on Velocity, Temperature and Skin Friction." Journal of Advanced Research in Computing and Applications 38, no. 1 (2025): 23-38.

[21] Ravikumar, V., M. C. Raju, and G. S. S. Raju. "Theoretical investigation of an unsteady MHD free convection heat and mass transfer flow of a non-Newtonian fluid flow past a permeable moving vertical plate in the presence of thermal diffusion and heat sink." International journal of engineering research in Africa 16 (2015): 90-109.

[22] Rabha, Kankana, and Shyamanta Chakraborty. "Unsteady MHD Free Convective Flow of a Micro-Polar Fluids Over a Vertical Porous Plate in the Presence of Radiation and Chemical Reaction." Heat Transfer 54, no. 4 (2025): 2443-2455.
[23] Lutera, Joseph Nicholaus, MN Raja Shekar, and B. Shankar Goud. "Radiation impact on heat and mass transfer of an unsteady MHD nanofluid flow past an exponentially accelerating vertical plate with heat generation." Radiation Effects and Defects in Solids 180, no. 9-10 (2025): 1270-1292.
[24] Sahu, Digbash, and Rudra Kanta Deka. "Combined impacts of thermal and mass stratification on unsteady MHD parabolic flow along an infinite vertical plate with periodic temperature variation and variable mass diffusion." Heat Transfer 54, no. 2 (2025): 1638-1649.
[25] Aroloye, Soluade Joseph, and Oluwalana Emmanuel Tope. "NUMERICAL SOLUTIONS OF HEAT AND MASS TRANSFER OF MAGNETOHYDRODYNAMIC FLOW OVER A VERTICAL PLATE IN THE PRESENCE OF HEAT DISSIPATION AND THERMAL RADIATION." The Journals of the Nigerian Association of Mathematical Physics 66 (2024): 27-38.
[26] Islam, Muhammad Minarul, and Riaz Hossain. "Heat and Mass Transfer in Unsteady MHD Casson Fluid Flow Over a Semi-Infinite Vertical Plate Through Porous Medium with Dissipative and Radiative Effects." Sciences 5 (2024): 6611-7687.
[27] Sudarmozhi, K., D. Iranian, and Qasem M. Al-Mdallal. "Revolutionizing energy flow: Unleashing the influence of MHD in the presence of free convective heat transfer with radiation." International Journal of Thermofluids 22 (2024): 100662.
[28] Das, Tusharkant, Tumbanath Samantara, Jayaprakash Mishra, and Sukanta Ku Sahoo. "Unsteady effects on MHD free convective flow over an infinite vertical porous plate with heat flux in presence of thermal radiation." In AIP Conference Proceedings, vol. 3081, no. 1, p. 050002. AIP Publishing LLC, 2024.
[29] Prakash, J., and A. Selvaraj. "Effects of radiation and heat generation on MHD and parabolic motion on Casson fluids flow through a rotating porous medium in a vertical plate." Journal of applied mathematics & informatics 42, no. 3 (2024): 607-623.
[30] Reddy, Y. Dharmendar, and B. Shankar Goud. "Comprehensive analysis of thermal radiation impact on an unsteady MHD nanofluid flow across an infinite vertical flat plate with ramped temperature with heat consumption." Results in Engineering 17 (2023): 100796.
[31] Hasanuzzaman, Md, Sathi Akter, Shanta Sharin, Md Mosharof Hossain, Akio Miyara, and Md Amzad Hossain. "Viscous dissipation effect on unsteady magneto-convective heat-mass transport passing in a vertical porous plate with thermal radiation." Heliyon 9, no. 3 (2023).
[32] Prabhakar Reddy, B., M. H. Simba, and Alfred Hugo. "Effects of thermo diffusion and chemical reaction on magnetohydrodynamic-radiated unsteady flow past an exponentially accelerated inclined permeable plate embedded in a porous medium." International Journal of Chemical Engineering 2023, no. 1 (2023): 9342174.
[33] Uddin, Mohammed Jahir, and Rehena Nasrin. "A numerical assessment of time-dependent magneto-convective thermal-material transfer over a vertical permeable plate." Journal of Applied Mathematics 2023, no. 1 (2023): 9977857.

[34] Sarma, Subhrajit, and Nazibuddin Ahmed. "Thermal diffusion effect on unsteady MHD free convective flow past a semi-infinite exponentially accelerated vertical plate in a porous medium." Canadian Journal of Physics 100, no. 10 (2022): 437-451.

[35] Poddar, Saykat, Muhammad Minarul Islam, Jannatul Ferdouse, and Md Mahmud Alam. "Steady-State Solution of MHD Heat and Mass Transfer Fluid Flow over a Semi-Infinite Vertical Plate in a Rotating System Dipped in a Porous Medium with Hall Current, Thermal Radiation, Heat Generation/Absorption and Joule Heating." International Journal of Heat & Technology 40, no. 2 (2022).